Journal of Organometallic Chemistry 758 (2014) 9–18

Contents lists available at ScienceDirect

Journal of Organometallic Chemistry

journal homepage: www.elsevier.com/locate/jorganchem

Synthesis, spectral and structural studies of silver and gold(I) complexes containing some symmetrical diphosphine ligands

Manoj Trivedi [a,*], Bhaskaran [a], Gurmeet Singh [a], Abhinav Kumar [b], Nigam P. Rath [c,**]

[a] Department of Chemistry, University of Delhi, Delhi 110007, India
[b] Department of Chemistry, University of Lucknow, Lucknow 226007, India
[c] Department of Chemistry & Biochemistry and Centre for Nanoscience, University of Missouri-St. Louis, One University Boulevard, St. Louis, MO 63121-4499, USA

ARTICLE INFO

Article history:
Received 28 January 2014
Accepted 31 January 2014

Keywords:
Diphosphine
Silver complex
Gold complex
X-ray
Weak interaction

ABSTRACT

New silver(I) and gold(I) complexes $[Ag_3(\mu_2\text{-}CN)_3(\kappa^2\text{-}P,P\text{-}dppf)_2]_n\cdot C_6H_{12}$ (**1**), $[Ag_4(\mu_2\text{-}CN)_4(\kappa^1\text{-}P,P\text{-}dtbpf)]_n$ (**2**), $[Au_2(\mu_1\text{-}CN)_2(\kappa^1\text{-}P,P\text{-}dppf)]$ (**3**), $[Au_2(\mu_1\text{-}CN)_2(\kappa^1\text{-}P,P\text{-}dtbpf)]$ (**4**), $[Ag_4(\mu_3\text{-}CN)_2(\mu_1\text{-}CN)_2(\kappa^1\text{-}P,P\text{-}dcpf)_2]$ (**5**), and $[Au_2(\mu_1\text{-}CN)_2(\kappa^1\text{-}P,P\text{-}dcpf)]$ (**6**) were prepared starting with MCN (M = Ag, Au) and dppf/dtbpf/dcpf (dppf = 1,1′-bis(diphenylphosphino) ferrocene; dtbpf = 1,1′-bis(di-*tert*-butylphosphino) ferrocene; dcpf = 1,1′-bis(dicyclohexylphosphino) ferrocene) in 1:1 M ratio in DCM:MeOH (50:50 V/V) at room temperature. The resulting complexes have been characterized by elemental analysis, IR, ^{1}H & ^{31}P NMR, ESI-MS and electronic absorption spectroscopy. Molecular structures for the complexes **1**, **2**, **5**, and **6** were determined crystallographically. Complex **1** and **2** exist as an infinite one-dimensional (1D) polymeric chain constructed by $[(\mu_2\text{-}CN)Ag(\mu_2\text{-}CN)Ag]$ fragments bridged *via* dppf/dtbpf ligands. The molecular structure of **5** reveals a centrosymmetric dimeric complex in which the two silver atoms are bonded to two dcpf ligands in κ^1 manner and two cyanide groups in a μ_3 bonding mode to generate nearly planar $Ag_2(\mu_3\text{-}CN)_2$ framework, while complex **6** exists in open bridging mode containing Au atoms in ideal linear coordination defined by *P,CN*-donor sets.

1. Introduction

Ferrocene-based phosphines have emerged as one of the most powerful classes of ligands in chiral and achiral catalysis [1–10]. Although there are many different types of ferrocenyl diphosphines, the most common are 1,1′-bis(diphenylphosphino) ferrocene (dppf) [11–25] and 1,1′-bis(di-*tert*-butylphosphino) ferrocene (dtbpf) [19,26]. These ligands have significant advantages over other diphosphines which contain alkyl, rather than metallocene, backbones [27]. There are several reports available on dppf [28–36] and a few on dtbpf [19,26,37–42] and dcpf [27,43]. Compared to the significant amount of work on dppf itself, dtbpf and dcpf have received surprisingly little attention. Recently another incentive to study silver and gold complexes of bis(phosphino)ferrocenes, are of particular interest on account of the potential of their compounds as biologically active agents [44], catalysts [45] and luminescent materials [46–49]. Previous work on the coinage metals, especially Ag^+, revealed a large variety of mono-, di- and polynuclear structures that can be assembled from dppf [3,28,29,50]. The structural outcome is generally hard to predict due to the numerous permutations arising from the flexible metal geometry (linear ↔ trigonal planar ↔ tetrahedral), dppf bonding (unidentate ↔ bridging ↔ chelating) and coordination state of the supporting anion (halide, pseudohalide etc.) (uncoordinated ↔ terminal ↔ bridging ↔ chelating ↔ capping). Our current understanding on $[AgX(dppf)]_n$ [29–31] and $[AuX(dppf)]_n$ [51–55] complexes is that they generally prefer dimeric and polymeric structures. Several variations are known depending on the interaction of the dppf and X^- but few reports are published till date related to dtbpf/dcpf and X^-. The dppf based complexes are commonly prepared from direct addition of MX to dppf using stoichiometric conditions of 1:1. During the course of our current study concerning interaction of MCN (M = Ag, Au) with dppf/dtbpf/dcpf, and to assist our understanding of the Ag(I) and Au(I) species present in solid and solution state, herein we report the synthesis, spectroscopic characterization, and structural studies of representative silver(I) and gold(I) complexes $[Ag_3(\mu_2\text{-}CN)_3(\kappa^2\text{-}P,P\text{-}dppf)_2]_n\cdot C_6H_{12}$ (**1**), $[Ag_4(\mu_2\text{-}CN)_4(\kappa^1\text{-}P,P\text{-}dtbpf)]_n$ (**2**)], $[Ag_4(\mu_3\text{-}$

* Corresponding author. Tel.: +91 (0) 9811730475.
** Corresponding author. Tel.: +1 314 516 5333.
E-mail addresses: manojtri@gmail.com (M. Trivedi), rathn@umsl.edu (N.P. Rath).

http://dx.doi.org/10.1016/j.jorganchem.2014.01.037
0022-328X/

CN)$_2$(μ_1-CN)$_2$(κ^1-*P,P*-dcpf)$_2$] (**5**) and [Au$_2$(μ_1-CN)$_2$(κ^1-*P,P*-dcpf)] (**6**), respectively.

2. Results and discussion

2.1. Synthesis

The reactions of silver(I) cyanide with 1,1′-bis(diphenylphosphino)ferrocene (dppf)/1,1′-bis(di-*tert*-butylphosphino) ferrocene (dtbpf)/1,1′-bis(dicyclohexylphosphino) ferrocene (dcpf) ligand in a dichloromethane:methanol mixture (50:50 V/V) in equimolar ratio under refluxing with stirring in dark afforded the infinite one dimensional polymeric chains [Ag$_3$(μ_2-CN)$_3$(κ^2-*P,P*-dppf)$_2$]$_n$·C$_6$H$_{12}$ (**1**), [Ag$_4$(μ_2-CN)$_4$(κ^1-*P,P*-dtbpf)]$_n$ (**2**) and centrosymmetric dimeric complex [Ag$_4$(μ_3-CN)$_2$(μ_1-CN)$_2$(κ^1-*P,P*-dcpf)$_2$] (**5**), respectively (Schemes 1–3), while the reactions of gold(I) cyanide with dppf/dtbpf/dcpf under the similar condition mention above in presence of light led to the isolation of binuclear gold(I) complexes [Au$_2$(μ_1-CN)$_2$(κ^1-*P,P*-dppf)] (**3**), [Au$_2$(μ_1-CN)$_2$(κ^1-*P,P*-dtbpf)] (**4**) and [Au$_2$(μ_1-CN)$_2$(κ^1-*P,P*-dcpf)] (**6**) (Schemes 1–3).

2.2. Characterization

All the complexes are air-stable, non-hygroscopic solids and soluble in dimethylformamide, dimethylsulfoxide and halogenated solvents but insoluble in petroleum ether and diethyl ether. The complexes were fully characterized by IR, UV–Vis, ^{1}H & ^{31}P NMR and ESI-MS. Analytical data of the complexes confirmed well to their respective formulations. More information about composition of the complexes was also obtained from ESI-MS. The positions of different peaks and overall fragmentation patterns in the ESI-MS of the respective complexes are consistent with their formulations. Infrared spectra of all the complexes exhibited characteristic band corresponding to $\nu_{C\equiv N}$ at 2136 cm^{-1}, 2114 cm^{-1}, 2138 cm^{-1}, 2151 cm^{-1}, 2129 cm^{-1} and 2147 cm^{-1}, respectively. However, only one $\nu_{C\equiv N}$ band agrees well with the presence of only one type of cyanide bridge between silver and gold (I) atom [58–62] which is in accordance with those reported in literature for bridging pseudo-halide groups [30,56–60]. The ^{1}H NMR spectra of all the complexes show two singlets in the range of $\delta = 4.43$–4.10 ppm corresponding to η^5-C$_5$H$_4$ protons of the dppf, dtbpf and dcpf ligand. The phenyl ring protons of dppf ligand in complex **1** and **3** resonated as a multiplets at $\delta = 8.10$–7.30 ppm. The *tert*-butyl protons in complex **2** and **4** were observed as two overlapping doublets at $\delta = 1.21$ ppm. The cyclohexyl proton in complex **5** and **6** were observed as multiplet at 2.71–1.22 ppm. The ^{31}P{^{1}H} NMR spectra for the complex **1**, **2**, and **5** resonated at δ −2.559 (**1**), 41.54 (**2**), and 56.6 (**5**) as a broad singlets, while the other complexes **3**, **4**, and **6** showed a single sharp resonance at δ 31.4 (**3**), 64.9 (**4**), and 41.6 ppm (**6**), respectively for dppf, dtbpf and dcpf ligands indicating that all the phosphorus atoms were chemically equivalent (See **F-1**–**F-3**, Supporting material). These chemical shifts are within the accepted range and are comparable to that of the silver(I) and gold(I) complexes containing dppf, dtbpf and dcpf ligands [27,28,30,32,33,35,37–43,61]. All the complexes exhibited two bands at 460–478 nm and 265–266 nm in dichloromethane solution (See **F-4**, Supporting material). The lower-energy band in the range of 460–478 nm can be assigned to the d–d transition

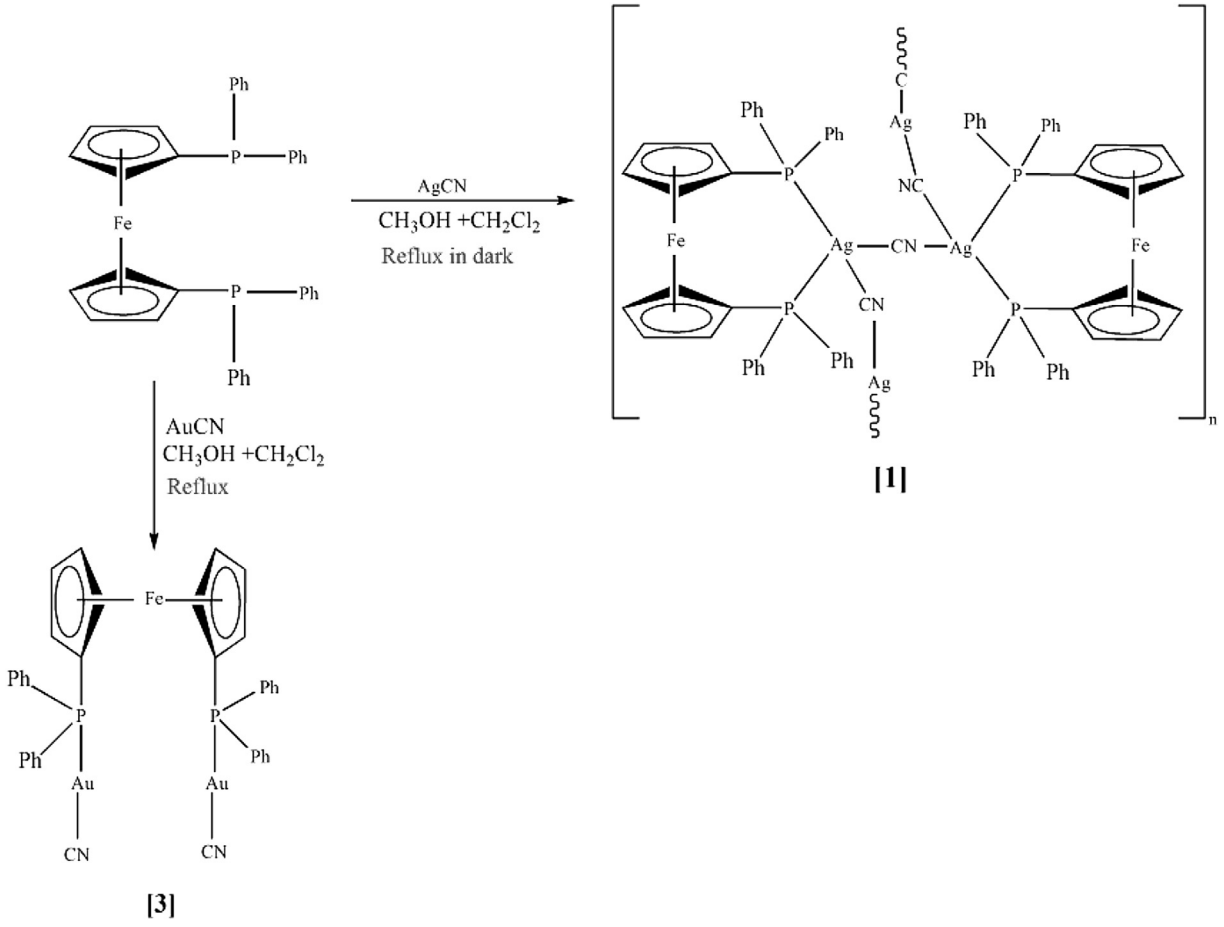

Scheme 1. Synthetic Routes for **1** and **3**.

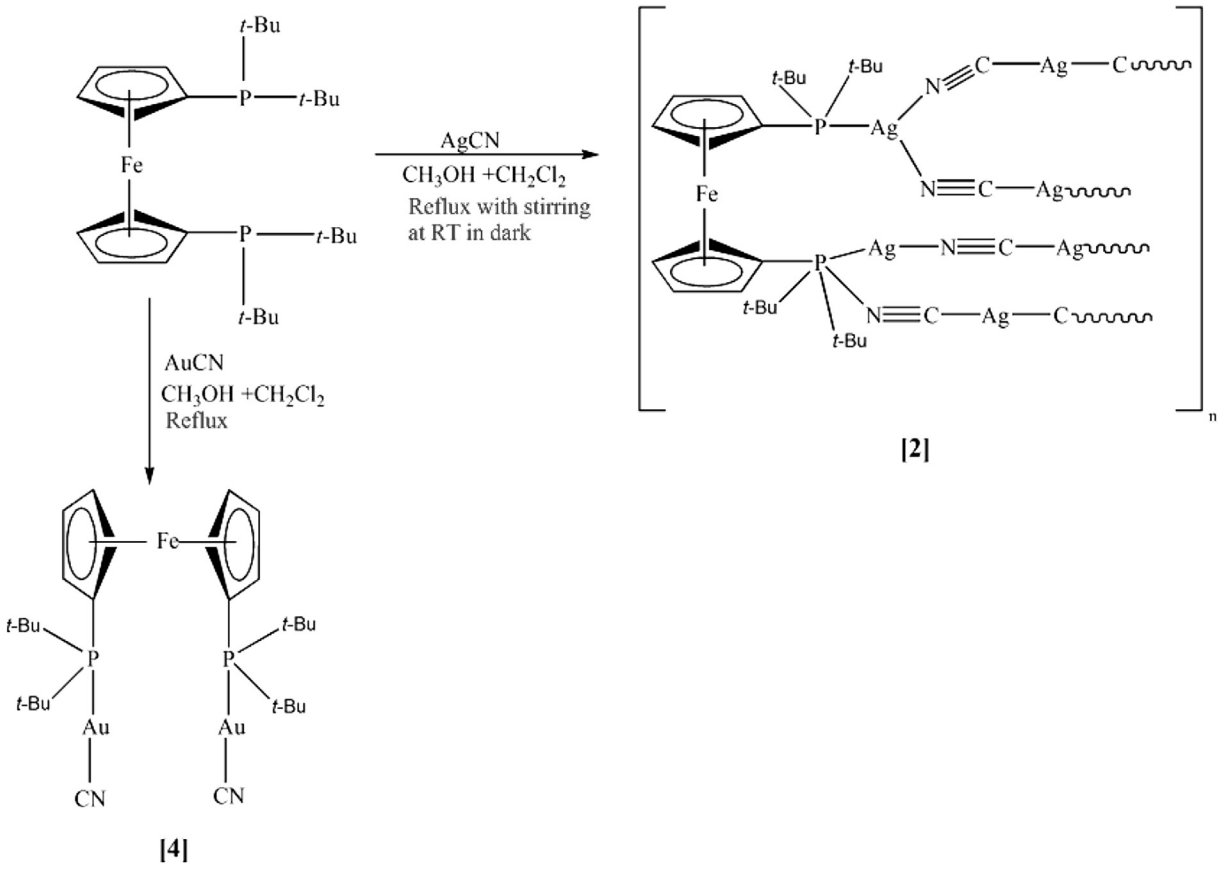

Scheme 2. Synthetic Routes for **2** and **4**.

assigned to the $^1E_{1g} \leftarrow {}^1A_{1g}$ of ferrocenyl moiety. The higher-energy band at 265–275 nm has been assigned to intraligand charge transfer.

2.3. Molecular structure determination

Details about the data collection, solution and refinement are presented in Table 1. The molecular structures for the complex **1**, **2**, **5** and **6** with atomic numbering scheme are presented in Figs. 1–4 and important geometrical and hydrogen bond parameters are presented in Tables 2 and 3, respectively. Complexes **1**, **2**, **5** and **6** crystallized in triclinic and monoclinic system with *P*-1, *C*2/c, *C*2/c and $P2_1/c$ space groups, respectively. The asymmetric unit of the complex **1** and **2** have one $[Ag_2(\mu_2\text{-}CN)_2Ag_1(\kappa^2\text{-}P,P\text{-dppf})]\cdot 0.5C_6H_{12}$ and $[Ag(\mu_1\text{-}CN)Ag(\mu_2\text{-}CN)(\kappa^1\text{-}P\text{-}0.5dtbpf)]$ molecules which propagated linearly to give an infinite one-dimensional zigzag and helical polymeric chains, while the molecular structure of **5** revealed a centrosymmetrical dimeric unit in which, the two dcpf ligands in κ^1 manner and two cyanide groups in μ_3 modes bridging the two silver atoms. The asymmetric unit of **6** comprises of binuclear $(C_{34}H_{52}FeP_2)(AuCN)_2$ molecule which is located at the inversion centre. As shown in Fig. 1, the two Ag atoms in complex **1** show different coordination geometries. The distorted tetrahedral coordination of Ag1 is achieved by two P atoms of the chelating dppf ligand [Ag(1)–P(1) = 2.4865(8) Å, Ag(1)–P(2) = 2.4588(8) Å] and two cyanide ligands [Ag(1)–N(1) = 2.313(3) Å, Ag(1)–C(35) = 2.200(14) Å, Ag(1)–N(35)$^{\#1}$ = 2.160(10) Å]. The bridging cyanide group around Ag1 in **1** is disordered across an inversion centre. The other Ag2 is linearly coordinated by two C atoms from two cyanides [Ag(2)–C(36) = 2.045(4) Å, Ag(2)–C(36)$^{\#1}$ = 2.045(4) Å, N(1)–C(36) = 1.114(5) Å]. The bond angles at Ag1 [N(1)–Ag(1)–P(1), C(35)–Ag(1)–N(1), C(35)–Ag(1)–P(2), N(1)–Ag(1)–P(2), C(35)–Ag(1)–P(1), and P(2)–Ag(1)–P(1)] lie in the range of 98.01(9)°–117.00(8)°. The Ag–P bonds are coplanar with the plane defined by the [Ag–CN–Ag–CN–]$_n$ zigzag backbone. The mean Ag–P, Ag–C(CN) and Ag1–N(CN) bond lengths (2.4727(8) Å *vs.* 2.0966(7) Å *vs.* 2.2365(7) Å) are longer than those of the $[\{Ag_2(CN)_2(dppmapy)\}\cdot 0.5CHCl_3]_n$ (where dppmapy: *N*-diphenylphosphanylmethyl-4-aminopyridine) (2.3880(19) Å *vs.* 2.062(9) Å *vs.* 2.217(5) Å) [57] but nearly similar as compared to $[P(o\text{-tol})_3Ag_2(CN)_2(py)]_n$ (2.451(2) Å *vs.* 2.3105 Å *vs.* 2.375(3) Å; *o*-tol = *o*-toluene) [62]. Complex **1** consists of $[(\mu_2\text{-}CN)Ag(\mu_2\text{-}CN)Ag]$ fragments bridged by the dppf ligands, forming an infinite 1D polymeric chain extending along the *b* axis (See **F-5**, Supporting material). The two substituted Cp rings in the dppf ligand in complex **1** adopt the antiperiplanar staggered conformation [Cp(centroid)···Fe···Cp(centroid) = 178.06°], which determines the conformational chirality of the Cp_2Fe fragment.

In complex **2**, the two Ag atoms are also in different coordination geometries (Fig. 2). Ag1 is disordered (disorder fraction is <10%) and almost in distorted trigonal planar environment, with the two cyanide ligands [Ag(1)–N(1) = 2.295(9) Å, Ag(1)–N(2) = 2.328(10) Å] in μ_2 mode and one phosphorous atom of dtbpf ligand in κ^1-manner [Ag(1)–P(1) = 2.4025(19) Å]. The other Ag2 is linearly coordinated by two C atoms from two cyanides [Ag(2)–C(14) = 2.043(12) Å, Ag(2)–C(15)$^{\#2}$ = 2.093(10) Å, N(2)–C(15) = 1.071(13) Å, N(1)–C(14) = 1.112(14) Å]. The bond angles at Ag1 [N(1)–Ag(1)–N(2), N(2)–Ag(1)–P(1), N(1)–Ag(1)–P(1)] lie in the range of 106.6(4)°-123.4(3)°, respectively. The Ag–P bonds are nearly perpendicular with the plane defined by the [Ag–CN–Ag–

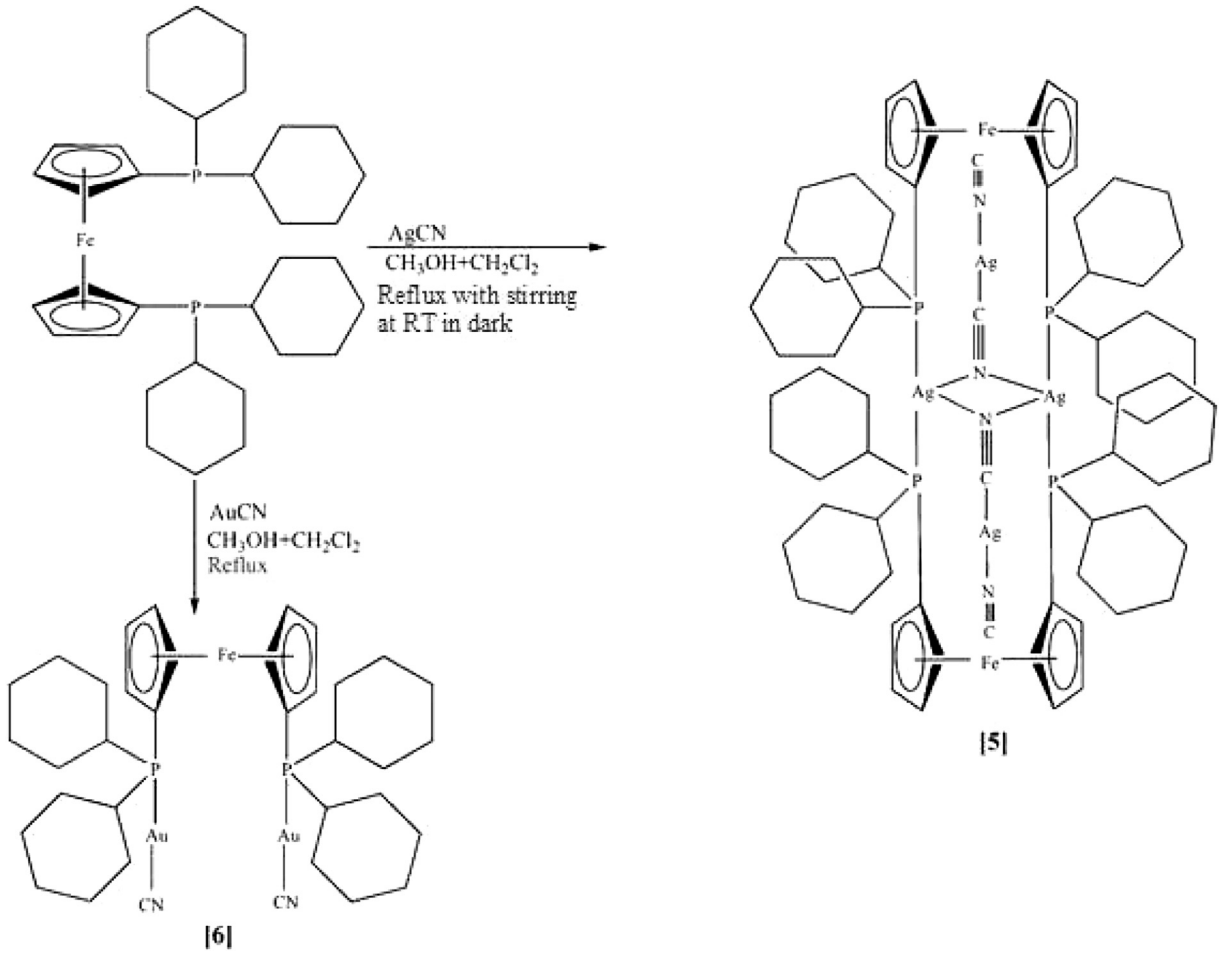

Scheme 3. Synthetic Routes for **5** and **6**.

CN−]$_n$ helical backbone. The mean Ag−P, Ag−C(CN) and Ag1−N(CN) bond lengths are (2.4025(19) Å *vs.* 2.068(11) Å *vs.* 2.312(10) Å). These distances are also longer than those of the [{$Ag_2(CN)_2$(dppmapy)}·0.5$CHCl_3$]$_n$ but nearly similar to [P(*o*-tol)$_3$-$Ag_2(CN)_2$(py)]$_n$ as observed above. The [(μ_2-CN)Ag(μ_2-CN)Ag] fragments bridged by the dtbpf ligands in complex **2**, resulting in the formation of an infinite 1D polymeric helical chain extending along the *b* axis (See **F-6**, Supporting material). The two substituted Cp rings in the dtbpf ligand in **2** adopt the antiperiplanar staggered conformation [Cp(centroid)···Fe···Cp(centroid) = 174.38°].

Table 1
Crystallographic data for **1**, **2**, **5** and **6**.

	1	**2**	**5**	**6**
Empirical Formula	$C_{77}H_{68}N_3P_4Ag_3Fe_2$	$C_{30}H_{44}N_4P_2Ag_4Fe$	$C_{72}H_{104}N_4P_4Ag_4Fe_2$	$C_{36}H_{52}N_2P_2Au_2Fe$
FW	1594.53	1009.96	1692.65	1024.52
Crystal system	Triclinic	Monoclinic	Monoclinic	Monoclinic
Space group	*P*-1	*C*2/c	*C*2/c	$P2_1/c$
a, Å	10.0301(4)	20.2238(10)	21.2347(6)	14.4052(3)
b, Å	13.5120(5)	10.4092(4)	14.2274(5)	9.5273(2)
c, Å	14.0645(5)	16.8208(8)	28.0768(10)	26.8320(5)
α, deg	117.245(4)	90.00	90.00	90.00
β, deg	97.598(3)	102.682(5)	106.418(3)	103.225(2)
γ, deg	96.137(3)	90.00	90.00	90.00
V, Å^3	1649.17(13)	3454.6(3)	8136.5(5)	3584.83(13)
Z	1	4	4	4
d_{calc}, g cm^{-3}	1.605	1.942	1.382	1.898
μ, mm^{-1}	1.448	2.756	1.408	8.681
T, K	293 (2)	293 (2)	150(2)	150(2)
R_1 all	0.0362	0.0615	0.0806	0.0429
R_1 [$I > 2\sigma(I)$]	0.0294	0.0552	0.0720	0.0379
wR_2	0.0827	0.1405	0.2322	0.0927
wR_2 [$I > 2\sigma(I)$]	0.0813	0.1358	0.2256	0.0898
GoF	1.090	1.078	1.112	1.137

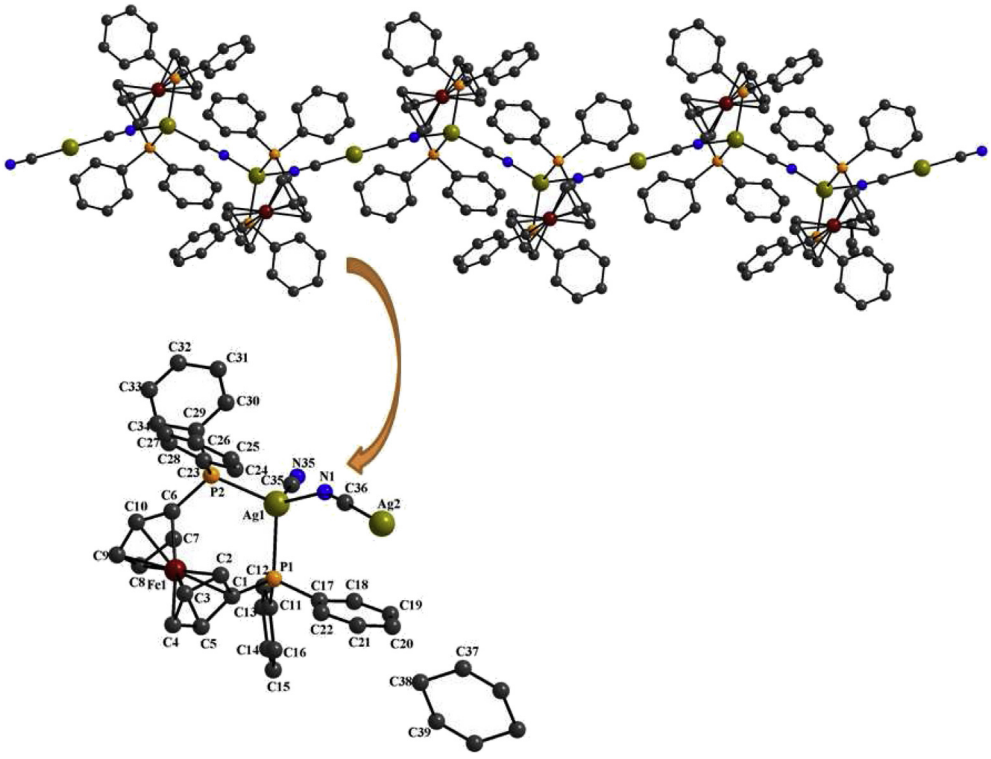

Fig. 1. Molecular structure for **1**.

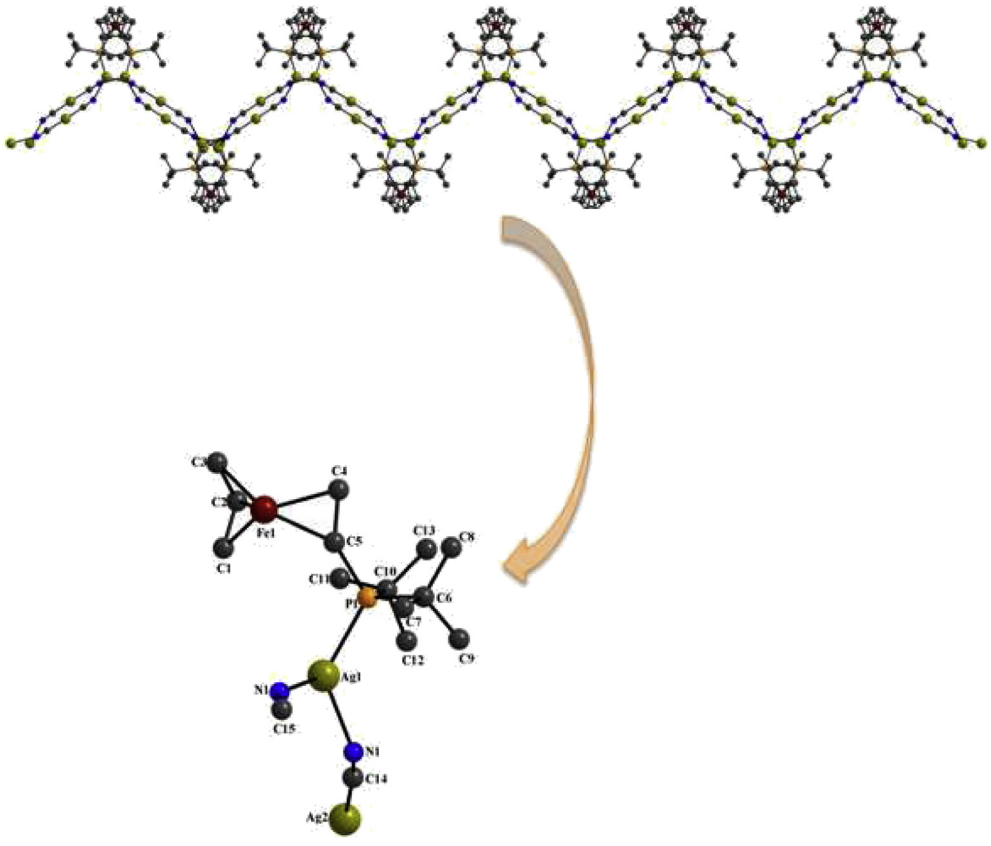

Fig. 2. Molecular structure for **2**.

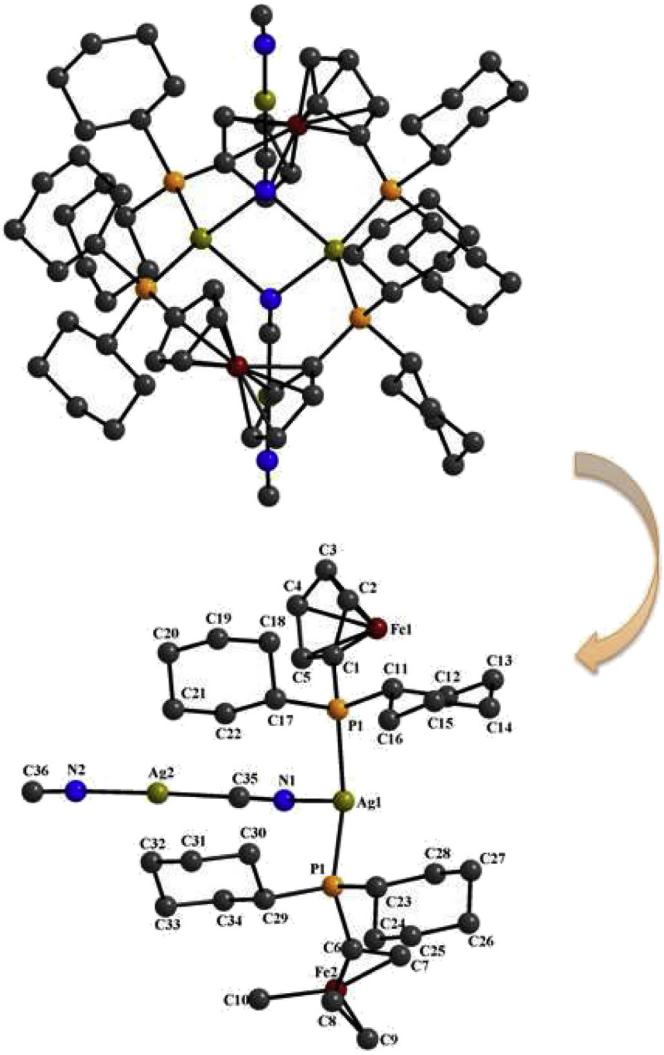

Fig. 3. Molecular structure for **5**.

In complex **5**, the two Ag atoms have different coordination geometries (Fig. 3). The distorted tetrahedral coordination of Ag1 is achieved by two P atoms of the chelating dcpf ligand [Ag(1)–P(1) = 2.443(2) Å, Ag(1)–P(2) = 2.442(2) Å] and two cyanide ligands [Ag(1)–N(1) = 2.510(7) Å, Ag(1)–N(1)$^{\#1}$ = 2.497(7) Å]. The other Ag2 is linearly coordinated by one C and one N atoms from two cyanides [Ag(2)–C(35) = 2.053(8) Å, Ag(2)–N(2) = 2.080(12) Å, C(36)–N(2) = 1.100(15) Å, N(1)–C(35) = 1.136(11) Å]. The P1–Ag–P2 bite angle for **5** is 130.00(7)°, of the chelating dcpf is very close to the expected value for this coordination. The other coordination bond angles in **5** are rather distorted [P(1)–Ag(1)–N(1) = 103.79(16), P(2)–Ag(1)–N(1) = 109.24(16), P(1)–Ag(1)–N(1)$^{\#1}$ = 110.72(16), P(2)–Ag(1)–N(1)$^{\#1}$ = 103.02(16), N(1)$^{\#1}$–Ag(1)–N(1) = 94.5(2)], because of the four-membered Ag_2N_2 ring and of the steric hindrance of the dcpf ligand. The two Ag–N bond lengths are asymmetrical, [2.497(7) and 2.510(7) Å]. The plane of the bridge defined in **5** by the two silver centres and the two nitrogen atoms is almost perpendicular to the plane defined by the four phosphorus atoms. The Ag···Ag distance in **5** is of 3.398(2) Å. The bond distances and angles in **5** agree with those reported bis(dicyclohexylphosphino) ferrocene complexes [27,43]. The two substituted Cp rings in the dcpf ligand in **5** adopt the antiperiplanar staggered conformation [Cp(centroid)···Fe···Cp(centroid) = 171.09°–177.16°], which determines the conformational chirality of the Cp_2Fe fragment.

In complex **6**, the iron atom lies on a symmetry centre. The dcpf ligand coordinates the gold centres in an open bridging mode (Fig. 4). The P1–Au1–C35 and P2–Au2–C36 bond angles are 178.9(3)°and 176.2(2)°, which is very close to the linear value. The Au–P and Au–C bond distances are 2.2634(18)–2.2674(17) Å and 1.989(8)–1.997(8) Å, respectively, which are comparable with other gold derivatives with ferrocenyl diphosphines [51–55]. The cyclopentadienyl ring is planar and located 1661–1.663 Å from the iron atom; by symmetry, both Cp rings are antiperiplanar staggered confirmation [Cp(centroid)···Fe···Cp(centroid) = 177.08°]. The shortest Fe–Au interactions [4.148–4.224 Å] are present in complex **6** (See **F-7**, Supporting material), and there is no short Au···Au contact (none <8.387 Å). Crystal packing in complex **1** and **6** are stabilised by inter- and intra-molecular C–H···X (X = N), C–H···π and π···π interactions, while in complex **2**, only inter- and intra-molecular C–H···π and intra π···π interactions are present. An interesting feature of the crystal packing in complex **1** is single helical motif resulting from inter and intra π···π interactions (See **F-8**, supporting material). The contact distances for π···π interactions are in the range of 3.211–3.378 Å. These distances are within the range reported previously [63]. Inter and intra-molecular C–H···N and C–H···π interactions are present in complex **1** and **6**, while in complex **2**, only C–H···π interactions are present. The contact distances for C–H···N and C–H···π interactions are in the range of 2.538–2.608 Å and 2.650–2.855 Å, respectively. These distances are within the range reported by other workers [64,65]. The self-assembling of **1**, **5** and **6** contains solvent accessible voids in the crystal 3D lattice, while no solvent accessible voids are present in the crystal 3D lattice of complex **2** (See **F-9**–**11**, Supporting material).

2.4. Electrochemistry

The electrochemical properties of our new complexes were investigated by cyclic voltammetry in CH_2Cl_2 at room temperature (r.t.) and the redox data are gathered in Table 4. Cyclic voltammograms (Fig. 5) of the complexes **1**, **2** and **5** exhibits two reversible oxidation peak at 0.19 V–0.77 V corresponding to $Fc^{+/0}$, and 0.76 V–1.26 V, which are due to Ag^{I}–Ag^{0} redox change of the silver-based units. We have also investigated the redox behaviour of the gold complexes **3**, **4**, and **6**. All show two reversible oxidation peaks at 0.21 V–0.25 V and 0.81 V–1.20 V, which could be tentatively assigned as arising from Fc^{+}/0, and Au^{I}–Au^{0} oxidation.

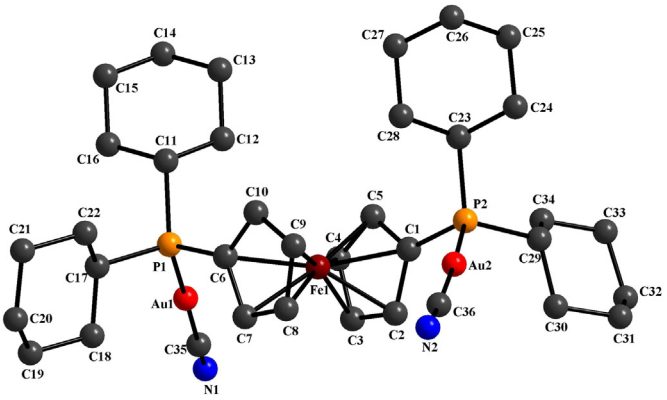

Fig. 4. Molecular structure for **6**.

Table 2
Selected bond lengths (Å), and bond angles (°) for **1**, **2**, **5** and **6**.

1		**2**		**5**		**6**	
Ag(1)–C(35)	2.200(14)	Ag(2)–C(14)	2.043(12)	C(36)–N(2)	1.100(15)	Au(2)–P(2)	2.2634(18)
Ag(1)–N(35)$^{\#1}$	2.160(10)	Ag(2)–C(15)$^{\#2}$	2.093(10)	Ag(1)–P(1)	2.443(2)	Au(1)–P(1)	2.2674(17)
Ag(1)–N(1)	2.313(3)	Ag(1)–N(1)	2.295(9)	Ag(1)–P(2)	2.442(2)	Au(2)–C(36)	1.997(8)
Ag(1)–P(2)	2.4588(8)	Ag(1)–N(2)	2.328(10)	Ag(1)–N(1)	2.510(7)	Au(1)–C(35)	1.989(8)
Ag(1)–P(1)	2.4865(8)	Ag(1)–P(1)	2.4025(19)	Ag(1)–N(1)$^{\#1}$	2.497(7)	P(1)–C(17)	1.835(6)
Ag(2)–C(36)	2.045(4)	N(1)–C(14)	1.112(14)	Ag(2)–C(35)	2.053(8)	P(1)–C(11)	1.849(6)
N(1)–C(36)	1.114(5)	N(2)–C(15)	1.071(13)	Ag(2)–N(2)	2.080(12)	P(2)–C(29)	1.849(6)
P(1)–C(17)	1.833(3)	P(1)–C(6)	1.893(7)	P(2)–C(23)	1.850(8)	P(2)–C(23)	1.834(7)
P(1)–C(11)	1.821(4)	P(1)–C(10)	1.882(7)	P(2)–C(29)	1.854(19)	N(2)–C(36)	1.135(10)
P(2)–C(23)	1.820(3)	N(1)–Ag(1)–N(2)	106.6(4)	P(1)–C(11)	1.852(8)	C(35)–N(1)	1.150(10)
P(2)–C(29)	1.831(3)	N(1)–Ag(1)–P(1)	123.4(3)	P(1)–C(17)	1.862(8)	N(1)–C(35)–Au(1)	176.5(8)
C(35)–Ag(1)–N(1)	117.0(19)	N(2)–Ag(1)–P(1)	121.1(2)	N(1)–C(35)	1.136(11)	N(2)–C(36)–Au(2)	177.3(8)
C(35)–Ag(1)–P(2)	111.00(3)	C(14)–Ag(2)–C(15)$^{\#2}$	178.1(5)	P(1)–Ag(1)–P(2)	130.00(7)	C(36)–Au(2)–P(2)	176.2(2)
N(1)–Ag(1)–P(2)	109.83(9)	N(1)–C(14)–Ag(2)	171.9(11)	P(1)–Ag(1)–N(1)	103.79(16)	C(35)–Au(1)–P(1)	178.9(3)
C(35)–Ag(1)–P(1)	112.00(3)			P(2)–Ag(1)–N(1)	109.24(16)		
N(1)–Ag(1)–P(1)	98.01(9)			P(2)–Ag(1)–N(1)$^{\#1}$	103.02(16)		
P(2)–Ag(1)–P(1)	108.84(3)			C(35)–Ag(2)–N(2)	178.50(4)		
C(36)$^{\#1}$–Ag(2)–C(36)	180.00(3)			Ag(1)$^{\#1}$–N(1)–Ag(1)	85.5(2)		
				N(1)–C(35)–Ag(2)	178.7(8)		
				C(36)–N(2)–Ag(2)	175.5(14)		

3. Conclusion

The work presented here concerns the reaction chemistry of silver(I) and gold(I) cyanide with dppf/dtbpf/dcpf ligands, that results in the formation of two infinite one dimensional silver(I) polymeric chains $[Ag_3(\mu_2\text{-}CN)_3(\kappa^2\text{-}P,P\text{-}dppf)_2]_n\cdot C_6H_{12}$ (**1**); $[Ag_4(\mu_2\text{-}CN)_4(\kappa^1\text{-}P,P\text{-}dtbpf)]_n$ (**2**), one centrosymmetric dimeric complex $[Ag_4(\mu_3\text{-}CN)_2(\mu_1\text{-}CN)_2(\kappa^1\text{-}P,P\text{-}dcpf)_2]$ (**5**) and three binuclear gold(I) complexes $[Au_2(\mu_1\text{-}CN)_2(\kappa^1\text{-}P,P\text{-}dppf)]$ (**3**), $[Au_2(\mu_1\text{-}CN)_2(\kappa^1\text{-}P,P\text{-}dtbpf)]$ (**4**) and $[Au_2(\mu_1\text{-}CN)_2(\kappa^1\text{-}P,P\text{-}dcpf)]$ (**6**), respectively. This result revealed that dppf/dtbpf/dcpf could be excellent ligands, and its chemistry related to metal cyanide is anticipated to be as rich as those of the other diphosphines. Further studies in this respect are underway in our laboratory.

4. Experimental

4.1. Materials and physical measurements

All the synthetic manipulations were performed under nitrogen atmosphere. The solvents were purified and dried before use by adopting the standard procedures [66]. Silver(I) cyanide, 1,1′-bis(-diphenylphosphino) ferrocene (Aldrich), gold(I) cyanide (Aldrich), 1,1′-bis(dicyclohexylphosphino)ferrocene (Aldrich) and 1,1′-bis(di-*tert*-butylphosphino) ferrocene (Aldrich) were used as received. Elemental analyses were performed on a Carlo Erba Model EA-1108 elemental analyzer and data of C, H and N is within ±0.4% of calculated values. Infrared spectra were recorded using Perkin–Elmer FT-IR spectrophotometer. Electronic spectra of the complexes were obtained on a Perkin Elmer Lambda-35 spectrometer. ^{1}H, and ^{31}P{^{1}H} NMR spectra were recorded on a JEOL AL-400 FTNMR instrument using tetramethylsilane and phosphoric acid as an internal standard, respectively. Mass spectral data were recorded using a Waters micromass LCT Mass Spectrometer/Data system. Electrochemical properties of the complexes were measured by cyclic voltammetry using platinum as working electrode and the supporting electrolyte was $[NBu_4]ClO_4$ (0.1 M) in dichloromethane solution of 0.001 M of complex versus Ag/AgCl at a scan rate of 100 mV s^{-1}.

4.2. Synthesis

4.2.1. $[Ag_3(\mu_2\text{-}CN)_3(\kappa^2\text{-}P,P\text{-}dppf)_2]_n\cdot C_6H_{12}$ (*1*)

1,1′-Bis(diphenylphosphino)ferrocene (dppf) (0.554 g, 1.0 mmol) was added to a solution of silver(I) cyanide (0.134 g, 1.0 mmol) in 30 mL CH_3OH:CH_2Cl_2 (50:50 V/V) mixture in dark at room temperature. The resultant suspension was refluxed with stirring under nitrogen atmosphere for 24 h. Slowly, the colour of the solution changed from light orange to dark yellowish orange. The resulting solution was evaporated to dryness to give a yellowish orange solid which was then extracted with dichloromethane (20 mL). The addition of cyclohexane (250 mL) to this solution led to yellowish orange needle shaped diffraction quality crystals. These were separated and washed with hexane and dried. Yield: (1.116 g, 70%). Anal. Calc. for $C_{77}H_{68}N_3P_4Ag_3Fe_2$: C, 57.97; H, 4.27; N, 2.63. Found: C, 58.12; H, 4.45; N, 2.68. IR (cm^{-1}, KBr): ν = 3440, 3052, 2926, 2136(CN), 1958, 1892, 1650, 1581, 1478, 1430, 1310, 1165, 1158, 1094, 1087, 1030, 898, 818, 742, 696, 630, 495. ^{1}H NMR (δ ppm, 400 MHz,

Table 4
Electrochemical data for **1**–**6** in dichloromethane solution/0.1 M $[NBu_4]ClO_4$ at 298 K.

Complex	Oxidation[a] E_{pa}/ V *vs.* SCE	Reduction[b] E_{pc}/ V *vs.* SCE
$[Ag_3(\mu_2\text{-}CN)_3(\kappa^2\text{-}P,P\text{-}dppf)_2]_n.C_6H_{12}$ (**1**)	0.77, 1.26	0.91, −0.13
$[Ag_4(\mu_2\text{-}CN)_4(\kappa^1\text{-}P,P\text{-}dtbpf)]_n$ (**2**)	0.19, 0.76	0.77, −0.46
$[Au_2(\mu_1\text{-}CN)_2(\kappa^1\text{-}P,P\text{-}dppf)]$ (**3**)	0.22, 0.95	−0.50, −1.13
$[Au_2(\mu_1\text{-}CN)_2(\kappa^1\text{-}P,P\text{-}dtbpf)]$ (**4**)	0.25, 1.20	−0.34, −1.03
$[Ag_4(\mu_3\text{-}CN)_2(\mu_1\text{-}CN)_2(\kappa^1\text{-}P,P\text{-}dcpf)_2]$ (**5**)	0.27, 0.89	0.77, −0.85
$Au_2(\mu_1\text{-}CN)_2(\kappa^1\text{-}P,P\text{-}dcpf)]$ (**6**)	0.21, 0.81	−0.18, 0.92

[a] E_{pa} is the anodic peak potential of the reversible oxidation wave.
[b] E_{pc} is the cathodic peak potential of the reversible oxidation wave.

Table 3
Hydrogen bond parameters for **1** and **6**.

D–H···A–X	*d* H···A Å	*D* D···A Å	*θ* D–H···A°
1			
C(9)–H(9)···N(1)[a]	2.54	3.416(5)	157
C(24)–H(24)···N(1)	2.61	3.499(5)	160
6			
C(11)–H(11)···N(2)[b]	2.53	3.440(4)	154
C(29)–H(29)···N(1)[c]	2.49	3.420(5)	157

Symmetry equivalents.
[a] 1 + *x*, *y*, *z*.
[b] −*x*, 1 − *y*, −*z*.
[c] 1 − *x*, 1 − y, −*z*.

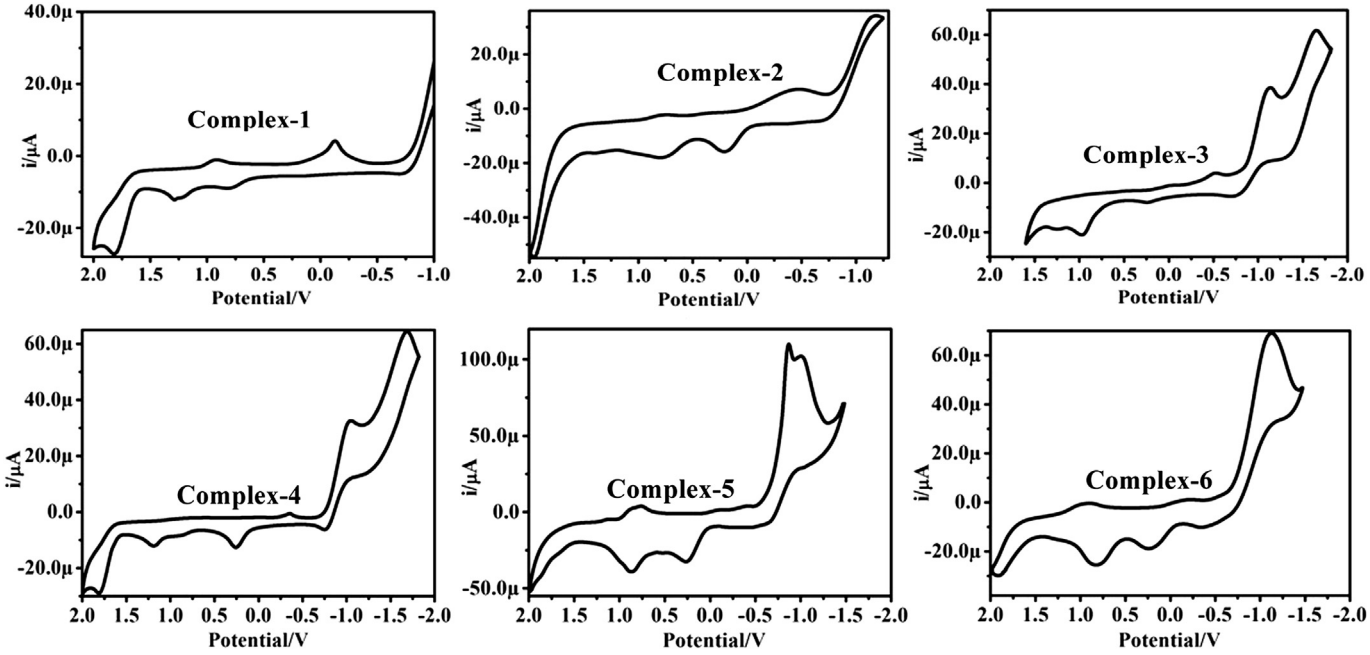

Fig. 5. Cyclic voltammograms for the complexes **1**–**6** in CH_2Cl_2/0.1 M $[NBu_4]ClO_4$ at 100 mV/s^{-1} scan rate.

$CDCl_3$, 298 K): 8.05–7.30 (m, 40H, Ph), 4.32(s, 8H, C_5H_4), 4.20 (s, 8H, C_5H_4). $^{31}P\{^1H\}$: δ −2.56 (sbr). UV/Vis: λ_{max} (ε [dm^3 mol^{-1} cm^{-1}]) = 266 (10,548), 460 (24,204). ESI-MS (*m*/*z*): 1594.1(M^+).

*4.2.2. $[Ag_4(\mu_2\text{-}CN)_4(\kappa^1\text{-}P,P\text{-}dtbpf)]_n$ (**2**)*

1,1′-Bis(di-*tert*-butylphosphino) ferrocene (dtbpf) (0.474 g, 1.0 mmol) was added to a solution of silver(I) cyanide (0.134 g, 1.0 mmol) in 30 mL CH_3OH:CH_2Cl_2 (50:50 V/V) mixture in dark at room temperature. The resultant suspension was refluxed with stirring under nitrogen atmosphere for 24 h. Slowly, the colour of the solution changed from light orange to dark yellowish red colour. The resulting solution was evaporated to dryness to give a yellowish red solid which was then extracted with dichloromethane (20 mL). The addition of hexane (100 mL) to this solution led to yellowish red rod shaped diffraction quality crystals. These were separated and washed with hexane and dried. Yield: (0.808 g, 80%). Anal. Calc. for $C_{30}H_{44}N_4P_2Ag_4Fe$: C, 35.64; H, 4.36; N, 5.54. Found: C, 35.82; H, 4.40; N, 5.64. IR (cm^{-1}, KBr): ν = 3410, 3095, 2987, 2947, 2899, 2867, 2718, 2459, 2114(CN), 1645, 1477, 1458, 1392, 1368, 1302, 1216, 1175, 1154, 1040, 1021, 932, 887, 812, 751, 663, 630. ^1H NMR (δ ppm, 400 MHz, $CDCl_3$, 298 K), 4.35(s, 4H, C_5H_4), 4.15 (s, 4H, C_5H_4), 1.21 (m, 36H, CH_3). $^{31}P\{^1H\}$: δ 41.54 (sbr). UV/Vis: λ_{max} (ε [dm^3 mol^{-1} cm^{-1}]) = 265 (20,432), 474 (18,890). ESI-MS (*m*/*z*): 1009.4 (M^+).

*4.2.3. $[Au_2(\mu_1\text{-}CN)_2(\kappa^1\text{-}P,P\text{-}dppf)]$ (**3**)*

1,1′-Bis(diphenylphosphino)ferrocene (dppf) (0.554 g, 1.0 mmol) was added to a solution of gold(I) cyanide (0.223 g, 1.0 mmol) in 30 mL CH_3OH:CH_2Cl_2 (50:50 V/V) mixture at room temperature. The resultant suspension was refluxed with stirring under nitrogen atmosphere for 24 h. Slowly, the colour of the solution changed from light yellowish orange to dark yellowish orange. The resulting solution was evaporated to dryness to give a dark yellowish orange solid which were separated and washed with hexane and dried. Yield: (0.500 g, 50%). Anal. Calc. for $C_{36}H_{28}N_2P_2Au_2Fe$: C, 43.20; H, 2.80; N, 2.80. Found: C, 43.32; H, 2.85; N, 2.91. IR (cm^{-1}, KBr): ν = 3430, 3022, 2929, 2147(CN), 1956, 1650, 1580, 1479, 1428, 1308, 1164, 1157, 1091, 1086, 1022, 890, 820, 740, 691, 630, 494. ^1H NMR (δ ppm, 400 MHz, $CDCl_3$, 298 K): 8.10–7.30 (m, 40H, Ph), 4.35(s, 8H, C_5H_4), 4.10 (s, 8H, C_5H_4). $^{31}P\{^1H\}$: δ 31.4 (s) (Sharp). UV/Vis: λ_{max} (ε [dm^3 mol^{-1} cm^{-1}]) = 275 (18,904), 450 (30,337). ESI-MS (*m*/*z*): 1000.8 (M^+).

*4.2.4. $[Au_2(\mu_1\text{-}CN)_2(\kappa^1\text{-}P,P\text{-}dtbpf)]$ (**4**)*

1,1′-Bis(di-*tert*-butylphosphino) ferrocene (dtbpf) (0.474 g, 1.0 mmol) was added to a solution of gold(I) cyanide (0.223 g, 1.0 mmol) in 30 mL CH_3OH:CH_2Cl_2 (50:50 V/V) mixture at room temperature. The resultant suspension was refluxed with stirring under nitrogen atmosphere for 24 h. Slowly, the colour of the solution changed from light yellowish orange to dark yellowish red colour. The resulting solution was evaporated to dryness to give a yellowish red solid which were separated and washed with hexane and dried. Yield: (0.598 g, 65%). Anal. Calc. for $C_{28}H_{44}N_2P_2Au_2Fe$: C, 36.52; H, 4.78; N, 3.04. Found: C, 36.62; H, 4.88; N, 3.24. IR (cm^{-1}, KBr): ν = 3404, 2930, 2940, 2878, 2861, 2151(CN), 1654, 1478, 1451, 1380, 1340, 1301, 1212, 1174, 1150, 1041, 1020, 930, 888, 810, 750, 664, 624. ^1H NMR (δ ppm, 400 MHz, $CDCl_3$, 298 K): 4.40(s, 4H, C_5H_4), 4.12 (s, 4H, C_5H_4), 1.22 (d, 36H, CH_3). $^{31}P\{^1H\}$: δ 64.9 (s) (Sharp). UV/Vis: λ_{max} (ε [dm^3 mol^{-1} cm^{-1}]) = 275 (15,932), 453 (41,573). ESI-MS (*m*/*z*): 920.5 (M^+).

*4.2.5. $[Ag_4(\mu_3\text{-}CN)_2(\mu_1\text{-}CN)_2(\kappa^1\text{-}P,P\text{-}dcpf)_2]$ (**5**)*

1,1′-Bis(dicyclohexylphosphino)ferrocene (dcpf) (0.578 g, 1.0 mmol) was added to a solution of silver(I) cyanide (0.134 g, 1.0 mmol) in 30 mL CH_3OH:CH_2Cl_2 (50:50 V/V) mixture at room temperature. The resultant suspension was refluxed with stirring under nitrogen atmosphere for 24 h in dark. Slowly, the colour of the solution changed from light yellowish orange to dark yellowish orange colour. The resulting solution was evaporated to dryness to give a yellowish orange solid which was then extracted with dichloromethane (20 mL). The addition of diethyl ether (100 mL) to this solution led to yellow needle shaped diffraction quality crystals. These were separated and washed with hexane and dried. Yield: (0.846 g, 50%). Anal. Calc. for $C_{72}H_{104}N_4P_4Ag_4Fe_2$: C, 51.06; H, 6.15; N, 3.31. Found: C, 51.28; H, 6.34; N, 3.43. IR (cm^{-1}, KBr): ν = 3401, 2926, 2852, 2368, 2345, 2129(CN), 1740, 1444, 1240, 1165,

1109, 1036, 850, 625, 480. ^{1}H NMR (δ ppm, 400 MHz, $CDCl_3$, 298 K): 4.43(s, 8H, C_5H_4), 4.18 (s, 8H, C_5H_4), 2.71–1.34 (m, 88H, Cy). ^{31}P{^{1}H}: δ 56.6 (sbr). UV/Vis: λ_{max} (ε [dm^3 mol^{-1} cm^{-1}]) = 272 (14,719), 478 (30,674). ESI-MS (m/z): 1692.8 (M^+).

4.2.6. [$Au_2(\mu_1$-CN)$_2(\kappa^1$-P,P-dcpf)] (**6**)

1,1′-Bis(dicyclohexylphosphino)ferrocene (dcpf) (0.578 g, 1.0 mmol) was added to a solution of gold(I) cyanide (0.223 g, 1.0 mmol) in 30 mL CH_3OH:CH_2Cl_2 (50:50 V/V) mixture at room temperature. The resultant suspension was refluxed with stirring under nitrogen atmosphere for 24 h. Slowly, the colour of the solution changed from light yellowish orange to dark yellowish orange colour. The resulting solution was evaporated to dryness to give a yellowish orange solid which was then extracted with dichloromethane (20 mL). The addition of hexane (100 mL) to this solution led to yellow needle shaped diffraction quality crystals. These were separated and washed with hexane and dried. Yield: (0.768 g, 75%). Anal. Calc. for $C_{36}H_{52}N_2P_2Au_2Fe$: C, 42.19; H, 5.08; N, 2.73. Found: C, 42.32; H, 5.32; N, 2.94. IR (cm^{-1}, KBr): ν = 3401, 2930, 2850, 2360, 2340, 2151(CN), 1730, 1440, 1240, 1164, 1110, 1032, 868, 630, 490. ^{1}H NMR (δ ppm, 400 MHz, $CDCl_3$, 298 K), 4.40(s, 4H, C_5H_4), 4.22 (s, 4H, C_5H_4), 2.71–1.22 (m, 44H, Cy). ^{31}P{^{1}H}: δ 41.6 (s) (Sharp). UV/Vis: λ_{max} (ε [dm^3 mol^{-1} cm^{-1}]) = 267 (10,727), 460 (23,595). ESI-MS (m/z): 1024.1 (M^+).

4.3. X-ray crystallographic study

The single crystal X-ray diffraction data for the complexes **1**, **2**, **5** and **6** were collected on an Oxford XCalibur CCD diffractometer equipped with graphite monochromatic Mo-Kα radiation (λ = 0.71073 Å) [67]. The frames for **1**, **2** and **5**, **6** were collected at 293(2) and 150(2) K. Intensity data were corrected for the Lorentz polarization effects, and an empirical absorption correction (SADABS) was also applied [68]. The structures were solved by the direct methods and refined by the full-matrix least-squares refinement techniques on F^2 using the program SHELXL-97 incorporated in the WINGX 1.70 crystallographic collective package [69]. The computer programme PLATON was used for analysing the interaction and stacking distances [70,71].

Acknowledgements

We gratefully acknowledge financial support by the Department of Science and Technology, New Delhi (Grant No. SR/FT/CS-104/2011). Special thanks are due to Professor Josef Michl, Department of Chemistry and Biochemistry, Colorado University, USA, Professor P. Mathur and Professor Shaikh M. Mobin, Indian Institute of Technology, Indore and National Single Crystal X-ray Diffraction Facility, Indian Institute of Technology, Mumbai for their kind encouragement and support.

Appendix A. Supplementary material

CCDC 872833, 924430, 949021, and 948922 contain the supplementary crystallographic data for this paper. These data can be obtained free of charge from The Cambridge Crystallographic Data Centre via www.ccdc.cam.ac.uk/data_request/cif.

Appendix B. Supplementary data

Supplementary data related to this article can be found at http://dx.doi.org/10.1016/j.jorganchem.2014.01.037.

References

[1] A. Togni, T. Hayashi (Eds.), Ferrocenes: Homogeneous Catalysis, Organic Synthesis, Materials Science, Wiley-VCH Verlag GmbH, Weinheim, Germany, 1995.
[2] J.J. Bishop, A. Davison, M.L. Katcher, D.W. Lichtenberg, R.E. Merrill, J.C. Smart, J. Organomet. Chem. 27 (1971) 241–249.
[3] G. Bandoli, A. Dolmella, Coord. Chem. Rev. 209 (2000) 161–196.
[4] T.J. Colacot, Chem. Rev. 103 (2003) 3101–3118.
[5] P. Štèpnićka, Eur. J. Inorg. Chem. 19 (2005) 3787–3803.
[6] R.G. Arrayás, J. Adrio, J.C. Carretero, Angew. Chem. Int. Ed. 45 (2006) 7674–7715.
[7] S.W. Chien, T.S.A. Hor, in: P. Štèpnićka (Ed.), Ferrocenes: Ligands, Materials and Biomolecules, John Wiley & Sons, Ltd., West Sussex, 2008, pp. 33–116.
[8] T.J. Colacot, S. Parisel, in: P. Štèpnićka (Ed.), Ferrocenes: Ligands, Materials and Biomolecules, John Wiley & Sons, Ltd., West Sussex, 2008, pp. 117–140.
[9] D.J. Young, S.W. Chien, T.S.A. Hor, Dalton Trans. 41 (2012) 12655–12665.
[10] J.-C. Hierso, R. Smaliy, R. Amardeil, P. Meunier, Chem. Soc. Rev. 36 (2007) 1754–1769.
[11] Z. Csok, O. Vechorkin, S.B. Harkins, R. Scopelliti, X. Hu, J. Am. Chem. Soc. 130 (2008) 8156–8157.
[12] S. Jamali, S.M. Nabavizadeh, M. Rashidi, Inorg. Chem. 47 (2008) 5441–5452.
[13] (a) A. Serra-Muns, A. Jutand, M. Moreno-Manas, R. Pleixats, Organometallics 27 (2008) 2421–2427;
(b) W.-Y. Wong, W.-T. Wong, K.-K. Cheung, J. Chem. Soc. Dalton Trans. (1995) 1379–1387.
[14] R. Kuwano, H. Kusano, Org. Lett. 10 (2008) 1979–1982.
[15] G.D. Vo, J.F. Hartwig, Angew. Chem. Int. Ed. 47 (2008) 2127–2130.
[16] M. Kawatsura, T. Hirakawa, T. Tanaka, D. Ikeda, S. Hayase, T. Itoh, Tetrahedron Lett. 49 (2008) 2450–2453.
[17] A.P. Shaw, H. Guan, J.R. Norton, J. Organomet. Chem. 693 (2008) 1382–1388.
[18] L.-C. Song, H.-T. Wang, J.-H. Ge, S.-Z. Mei, J. Gao, L.-X. Wang, B. Gai, L.-Q. Zhao, J. Yan, Y.-Z. Wang, Organometallics 27 (2008) 1409–1416.
[19] N. Fey, J.N. Harvey, G.C. Lloyd-Jones, P. Murray, A.G. Orpen, R. Osborne, M. Purdie, Organometallics 27 (2008) 1372–1383.
[20] T. Dahl, C.W. Tornoee, B. Bang-Andersen, P. Nielsen, M. Joergensen, Angew. Chem. Int. Ed. 47 (2008) 1726–1728.
[21] B.-T. Guan, S.-K. Xiang, B.-Q. Wang, Z.-P. Sun, Y. Wang, K.-Q. Zhao, Z.-J. Shi, J. Am. Chem. Soc. 130 (2008) 3268–3269.
[22] T. Jensen, H. Pedersen, B. Bang-Andersen, R. Madsen, M. Joergensen, Angew. Chem. Int. Ed. 47 (2008) 888–890.
[23] J. Arias, M. Bardaji, P. Espinet, Inorg. Chem. 47 (2008) 1597–1606.
[24] W.-Y. Wong, F.-L. Ting, W.-L. Lam, Eur. J. Inorg. Chem. (2002) 2103–2111.
[25] W.-Y. Wong, G.-L. Lu, K.-H. Choi, J. Organomet. Chem. 659 (2002) 107–116.
[26] K.M. Clapham, A.S. Batsanov, R.D.R. Greenwood, M.R. Bryce, A.E. Smith, B. Tarbit, J. Org. Chem. 73 (2008) 2176–2181.
[27] L.E. Hagopian, A.N. Campbell, J.A. Golen, A.L. Rheingold, C. Nataro, J. Organomet. Chem. 691 (2006) 4890–4900.
[28] X.L. Lu, W.K. Leong, T.S.A. Hor, L.Y. Goh, J. Organomet. Chem. 689 (2004) 1746–1756.
[29] S.P. Neo, T.S.A. Hor, Z.Y. Zhou, T.C.W. Mak, J. Organomet. Chem. 464 (1994) 113–119.
[30] C.D. Nicola Effendy, C. Pettinari, B.W. Skelton, N. Somers, A.H. White, Inorg. Chim. Acta 358 (2005) 695–706.
[31] P. Teo, L.L. Koh, T.S.A. Hor, Chem. Commun. (2007) 4221–4223.
[32] C.D. Nicola Effendy, C. Pettinari, B.W. Skelton, A.H. White, Inorg. Chim. Acta 359 (2006) 2170–2177.
[33] X.L. Lu, W.K. Leong, L.Y. Goh, T.S.A. Hor, Eur. J. Inorg. Chem. (2004) 2504–2513.
[34] M.C. Gimeno, P.G. Jones, A. Laguna, C. Sarroca, J. Chem. Soc. Dalton Trans. (1995) 1473–1481.
[35] T.S.A. Hor, J.S.P. Neo, C.S. Tan, T.C.W. Mak, K.W.P. hung, R.-J. Wang, Inorg. Chem. 31 (1992) 4510–4516.
[36] J.H.K. Yip, J. Wu, K.-Y. Wong, K.-W. Yeung, J.J. Vittal, Organometallics 21 (2002) 1612–1621.
[37] M.A. Zuideveld, B.H.G. Swennenhuis, P.C.J. Kamer, P.W.N.M. van Leeuwen, J. Organomet. Chem. 637–639 (2001) 805–808.
[38] W.R. Cullen, T.-J. Kim, F.W.B. Einstein, T. Jones, Organometallics 2 (1983) 714–719.
[39] J.H.L. Ong, C. Nataro, J.A. Golen, A.L. Rheingold, Organometallics 22 (2003) 5027–5032.
[40] G. Grasa, T.J. Colacot, Org. Lett. 9 (2007) 5489–5492.
[41] G. Mann, Q. Shelby, A.H. Roy, J.F. Hartwig, Organometallics 22 (2003) 2775–2789.
[42] F.N. Blanco, L.E. Hagopian, W.R. McNamara, J.A. Golen, A.L. Rheingold, C. Nataro, Organometallics 25 (2006) 4292–4300.
[43] J. Berstler, A. Lopez, D. Ménard, W.G. Dougherty, W.S. Kassel, A. Hansen, A. Daryaei, P. Ashitey, M.J. Shaw, N. Fey, C. Nataro, J. Organomet. Chem. 712 (2012) 35–45.
[44] S.J. Berners-Price, R.J. Bowen, P. Galettis, P.C. Healy, M.J. McKeage, Coord. Chem. Rev. 823 (1999) 185–186.
[45] M. Ohkouchi, D. Masui, M. Yamaguchi, T. Yamagishi, J. Mol. Catal. A: Chem. 170 (2001) 1–16.

[46] D. Sun, R. Cao, J. Weng, M. Hong, Y. Liang, J. Chem. Soc. Dalton Trans. (2002) 291–292.
[47] C.-M. Che, M.-C. Tse, M.C.W. Chan, K.-K. Cheung, D.L. Philips, K.-K. Leung, J. Am. Chem. Soc. 122 (2000) 2464–2468.
[48] M.-C. Brandys, M.C. Jennings, R.J. Puddephatt, J. Chem. Soc. Dalton Trans. (2000) 4601–4606.
[49] M.J. Irwin, J.J. Vittal, R.J. Puddephatt, Organometallics 16 (1997) 3541–3547.
[50] R. Horikoshi, T. Mochida, Eur. J. Inorg. Chem. (2010) 5355–5371.
[51] A. Houlton, D.M.P. Mingos, D.M. Murphy, D.J. Williams, L.-T. Phang, T.S.A. Hor, J. Chem. Soc. Dalton Trans. (1993) 3629–3630.
[52] N. Meyer, F. Mohr, E.R.T. Tiekink, Acta Crystallogr. E66 (2010) m168–m169.
[53] M.C. Gimeno, A. Laguna, C. Sarroca, P.G. Jones, Inorg. Chem. 32 (1993) 5926–5932.
[54] F. Canales, M.C. Gimeno, P.G. Jones, A. Laguna, C. Sarroca, Inorg. Chem. 36 (1997) 5206–5211.
[55] L.-T. Phang, T.S.A. Hor, Z.-Y. Zhou, T.C.W. Mak, J. Organomet. Chem. 469 (1994) 253–261.
[56] H.-X. Zhang, B.-S. Kang, L.-R. Deng, C. Ren, C.-Y. Su, Z.-N. Chen, Inorg. Chem. Commun. 4 (2001) 41–44.
[57] N.-Y. Li, Z.-G. Ren, D. Liu, R.-X. Yuan, L.-P. Wei, L. Zhang, H.-X. Li, J.-P. Lang, Dalton Trans. 39 (2010) 4213–4222.
[58] A.J. Deeming, G.P. Proud, H.M. Daves, M.B. Hursthouse, Polyhedron 7 (1988) 651–657.
[59] C.A. Bayse, J.L. Ming, K.M. Miller, S.M. McCollough, R.D. Pike, Inorg. Chim. Acta 375 (2011) 47–52.
[60] R.L. White-Morris, M. Stender, D.S. Tinti, A.L. Balch, D. Rios, S. Attar, Inorg. Chem. 42 (2003) 3237–3244.
[61] P. Teo, L.L. Koh, T.S.A. Hor, Inorg. Chem. 47 (2008) 9561–9568.
[62] G.A. Bowmaker Effendy, J.C. Reid, C.E.F. Rickard, B.W. Skelton, A.H. White, J. Chem. Soc. Dalton Trans. (1998) 2139–2146.
[63] E.A. Meyer, R.K. Castellano, F. Diederich, Angew. Chem. Int. Ed. Engl. 42 (2003) 1210–1250.
[64] D. Braga, F. Grepioni, E. Tedesco, Organometallics 17 (1998) 2669–2672.
[65] D. Braga, P.J. Dyson, F. Grepioni, B.F.G. Johnson, Chem. Rev. 94 (1994) 1585–1620.
[66] B.S. Furniss, A.J. Hannaford, V. Rogers, P.W.G. Smith, A.R. Tatchell, Vogel's Textbook of Practical Organic Chemistry, fourth ed, Longman, London, 1978.
[67] CrysAlisPro, Oxford Diffraction Ltd., 2009. Version 1.171.33.49b.
[68] SHELXTL-NT, Version 6.10, Bruker Analytical X-ray System, Madison, WI, 2000.
[69] L.J. Farrugia, WinGX Version 1.70, An Integrated System of Windows Programs for the Solution, Refinement and Analysis of Single-Crystal X-ray Diffraction Data, Department of Chemistry, University of Glasgow, 2003.
[70] G.M. Sheldrick, SHELX-97; Programme for Refinement of Crystal Structures, University of Gottingen, Gottingen, Germany, 1997.
[71] PLATON A.L. Spek, Acta Crystallogr. 46A (1990) C34.